

Transport Properties in Dense QCD Matter

Toshitaka Tatsumi ^{1,*} and Hiroaki Abuki ² ¹ Institute of Education, Osaka Sangyo University, 3-1-1 Nakagaito, Daito, Osaka 574-8530, Japan² Department of Physics, Aichi University of Education, Hirosawa 1, Kariya 448-8542, Japan; abuki@aecc.aichi-edu.ac.jp

* Correspondence: tatsumitoshitaka@gmail.com

Received: 6 February 2020; Accepted: 27 February 2020; Published: 2 March 2020



Abstract: Transport properties of dense QCD matter are discussed. Using the Kubo formula for conductivity, we discuss some topological aspects of quark matter during the chiral transition. The close relation to Weyl semimetal is pointed out and anomalous Hall effect is demonstrated to be possible. In particular, it is shown that the spectral asymmetry of the quasi-particles plays an important role for the Hall conductivity in the magnetic field.

Keywords: chiral transition; inhomogeneous chiral phase; anomalous Hall effect; Weyl semimetal; spectral asymmetry

1. Introduction

Recently, much effort has been made theoretically or experimentally to explore the QCD phase diagram in the temperature–density plane [1], where various phase transitions have been proposed. Among them, deconfinement transition and chiral transition are fundamental subjects for QCD. Phenomenologically these transitions may affect the evolution of the universe or physics of compact stars. We, hereafter, consider the chiral transition mainly at low-temperature.

Many studies have shown that the chiral transition from the spontaneously symmetry-broken (SSB) phase to the quark-gluon plasma (QGP) phase should be present at some density and temperature, using the effective models of QCD, while at the moment it has not yet been directly proven from the first principle computations with lattice gauge theory due to the sign problem [2]. Recently, the possible appearance of the inhomogeneous chiral phase (iCP) has been suggested near the chiral transition, and extensively studied in various situations, including in the presence of magnetic field [3–8].

Here, we reveal a new aspect of the iCP in relation to Weyl semimetal (WSM) in condensed-matter physics [9]. We focus on the transport properties in the iCP to reveal some topological features inherent in the iCP. First, we shall see that the energy spectrum of quasi-particles in the iCP phase is the same as WSM, and the anomalous Hall effect (AHE) [10,11] also works in iCP. In this case, the AHE is brought about by the magnetic monopole in the momentum space. Next, we consider the Hall conductivity in the presence of magnetic field. This subject is important to understand the transport properties inside compact stars, such as thermal evolution of magnetars [12]. In condensed-matter physics, this subject has been also discussed to elucidate the transport properties of topological materials [13]. We shall see that anomalous Hall conductivity also appears as the magnetic-field-independent term due to the spectral asymmetry. Thus, the competition between AHE and the usual Hall effect is interesting as the strength of magnetic field increases.

2. Inhomogeneous Chiral Phase in Dense QCD and Weyl Semimetal

2.1. Dual Chiral Density Wave

iCP is characterized by the generalized order parameter,

$$\chi(\mathbf{r}) \equiv \langle \bar{\psi}\psi \rangle + i\langle \bar{\psi}i\gamma_5\tau_3\psi \rangle = \Delta(\mathbf{r}) \exp(i\theta(\mathbf{r})), \quad (1)$$

for the symmetry breaking of $SU(2)_L \times SU(2)_R$. The order parameters Δ , θ are now spatially dependent, and various types of $\chi(\mathbf{r})$ can be chosen, depending on the situation [6].

The dual chiral density wave (DCDW) is a kind of density wave and the DCDW phase is specified by the scalar and pseudoscalar condensates with spatial modulation [3],

$$\begin{aligned} \langle \bar{\psi}\psi \rangle &= \Delta \cos(\mathbf{q}\cdot\mathbf{r}), \\ \langle \bar{\psi}i\gamma_5\tau_3\psi \rangle &= \Delta \sin(\mathbf{q}\cdot\mathbf{r}). \end{aligned} \quad (2)$$

The order parameters are the amplitude Δ and the wavevector \mathbf{q} . We, hereafter, focus on this type, because the phase degree of freedom is indispensable for manifestation of topological effects in iCP. Moreover, it may be the most favorable configuration in the presence of the magnetic field [6–8].

We take the Nambu–Jona-Lasinio (NJL) model as an effective model of QCD at a low-energy scale:

$$L_{\text{NJL}} = \psi(i\partial - m_c)\psi + G\left[\langle \bar{\psi}\psi \rangle^2 + \langle \bar{\psi}i\gamma_5\tau_3\psi \rangle^2\right]. \quad (3)$$

We, hereafter, consider the flavor symmetric u and d quark matter in the chiral limit $m_c = 0$. Then, the effective Lagrangian can read under the mean-field approximation as follows:

$$\begin{aligned} L_{\text{MF}} &= \bar{\psi}\left(i\partial - \frac{1+\gamma_5\tau_3}{2}M(z) - \frac{1-\gamma_5\tau_3}{2}M^*(z)\right)\psi - \frac{|M(z)|^2}{4G}, \\ M(z) &= -2G\Delta e^{iqz} (\equiv Me^{iqz}). \end{aligned} \quad (4)$$

One may rewrite it in a simple form,

$$L_{\text{MF}} = \bar{\psi}_W[i\partial - M - 1/2\gamma_5\tau_3q]\psi_W - G\Delta^2, \quad (5)$$

where $M = -2G\Delta$ and the spacelike vector $q^\mu = (0, \mathbf{q})$ by the use of the Weinberg transformation, $\Psi_W = \exp[i\gamma_5\tau_3\mathbf{q}\cdot\mathbf{r}/2]$. Thus, we can see that the amplitude of the DCDW provides the dynamical mass for the newly defined quarks (quasi-particles) described by Ψ_W , while the wavevector plays the role of the mean-field for them. The effective Hamiltonian operator in the momentum space then renders:

$$H_{\text{MF}}(\mathbf{p}) = \begin{pmatrix} M + \tau_3/2\sigma\cdot\mathbf{q} & \sigma\cdot\mathbf{p} \\ \sigma\cdot\mathbf{p} & -M + \tau_3/2\sigma\cdot\mathbf{q} \end{pmatrix}. \quad (6)$$

The single-particle energy can be easily extracted,

$$E_{\varepsilon=\pm 1, s=\pm 1}(p) = \varepsilon \sqrt{E_p^2 + |\mathbf{q}|^2/4 + s\sqrt{(\mathbf{p}\cdot\mathbf{q})^2 + M^2|\mathbf{q}|^2}}, \quad (7)$$

with $E_p = \sqrt{p^2 + M^2}$ for each flavor, where ε and s denote the particle-antiparticle and spin degrees of freedom, respectively. Accordingly, this form suggests anisotropy of the Fermi sea in the momentum space: it deforms in an axial-symmetric way around the direction of \mathbf{q} .

Thermodynamic potential can be easily evaluated for given temperature T and baryon number chemical potential μ , using the single-particle energy (7). Then, the values of the order parameters can be easily extracted: we can see that the DCDW phase appears around several times the normal nuclear density at $T = 0$ (see Figure 1a), where the usual chiral transition has been expected [3]. It should be

interesting to see that the value of the wavevector becomes rather high, $\frac{q}{2} = O(\mu) > M$ (Figure 1b), which is reminiscent of the nesting effect of the Fermi surface. Actually, it has been

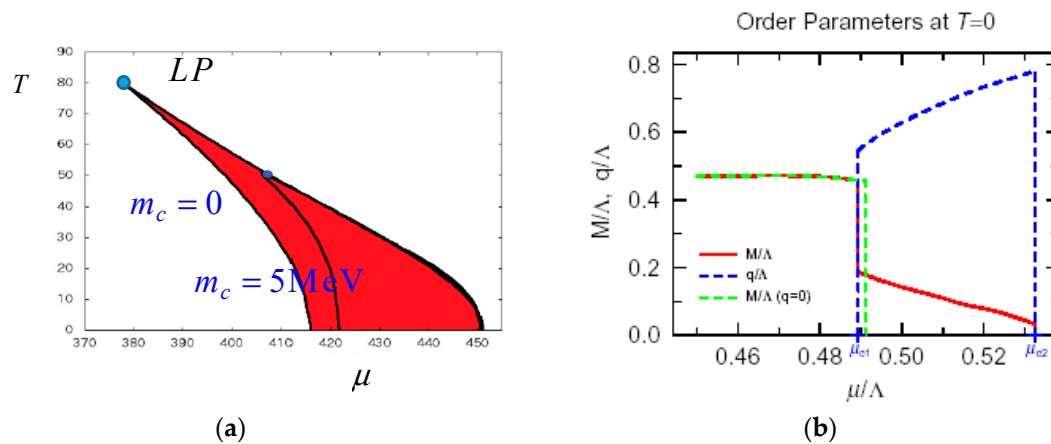


Figure 1. (a) QCD phase diagram including the dual chiral density wave (DCDW) phase in the density–temperature plane from Karasawa and Tatsumi [14]. The triple point LP is called the Lifshitz point, where the spontaneously symmetry-broken (SSB) phase, the QGP phase, and iCP coexist. (b) Density dependence of the order parameters in the unit of the cut-off parameter Λ , from Nakano and Tatsumi [3]. The dynamical mass in the usual chiral transition is also depicted by M/Λ ($q = 0$). Here we take $q = (0, 0, q)$, $q > 0$.

Shown that the DCDW phase is always favored by the nesting effect at one plus one dimensions [15,16]. We also anticipate that the appearance of the phase with spatially modulating order should be a rather universal phenomenon during the phase transitions both described by the uniform order parameter such as FFLO state in the context of superconductivity [17,18].

2.2. Similarity with Weyl Semimetal

The energy spectrum for $s = 1$ has a gap between positive and negative energies in momentum space. On the other hand, the energy spectrum for $s = -1$ exhibits an interesting behavior, depending on the values of q and M ; for $q/2 < M$ there is an energy gap, while there is no energy gap at the points, $\mathbf{p} = (0, 0, \pm K_0)$, with $K_0 = \sqrt{(q/2)^2 - M^2}$ for the opposite case, $q/2 > M$. These points are called Weyl points in condensed-matter physics and the quasi-particle excitations can be expressed by the use of the 2×2 Weyl Hamiltonian around these points. The latter case is actually realized in the DCDW phase. In Figure 2, we sketch the energy surface for $s = -1$ and $q/2 > M$.

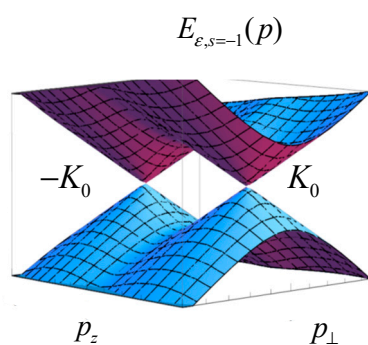


Figure 2. Schematic view of the energy surface of the quasi-particles with $s = -1$ in the momentum space. The Weyl points are located at $\pm K_0$ on the p_z axis, around which the excitations of the quasi-particles are described by the Weyl Hamiltonian.

Here we point out a similarity to Weyl semimetal. WSM is one of the topological materials and can be modeled by the Dirac type Hamiltonian [9],

$$H_{\text{WSM}}(\mathbf{k}) = \begin{pmatrix} m + b\sigma_z & \mathbf{k} \cdot \boldsymbol{\sigma} \\ \mathbf{k} \cdot \boldsymbol{\sigma} & -m + b\sigma_z \end{pmatrix}, \quad (8)$$

where \mathbf{k} denotes the Bloch momentum, and m is the spin-orbit coupling strength. The parameter b in the CPT-violating term controls the spin-splitting due to magnetic impurities doped in the materials. Thus, one may immediately notice that Hamiltonian Equation (8) has the same structure as Equation (6) for the DCDW case; b corresponds to $q/2$. Some remarks are in order here: first, the parameter m can take $m = 0$ without any inconsistency, in highly contrast to the DCDW phase, where $M = 0$ implies no phase transition. Secondly, only the negative energy states (valence band) are occupied in WSM, while some Fermi sea (conduction band) is formed in the DCDW phase. Thirdly, there is a boundary in the WSM.

This is a new encounter of nuclear physics and condensed-matter physics in the context of compact stars. One may extract some hints or suggestions to transport properties in dense quark matter by way of studies of topological materials such as WSM.

3. Anomalous Hall Effect in iCP

3.1. Hall Conductivity

Once we notice similarities with WSM, what can we learn about the DCDW phase? We, hereafter, examine the possible anomalous Hall effect in the DCDW phase. When magnetic field is applied, off-diagonal resistivity $\rho_{xy} \propto [\sigma^{-1}]_{xy}$ is generally expressed as $\rho_{xy} = R_0 B_z + R_s M_z$ with magnetization \mathbf{M} . The first term is a usual one representing the Hall effect, while the second term implies that the Hall effect occurs without any magnetic field. Such an effect is called the anomalous Hall effect [9,10]. AHE provides firm experimental evidence of WSM [9]. It may affect the transport properties through modification of the Maxwell equations [19,20]. Its phenomenological implications should also be interesting for compact stars. In the following, we would like to demonstrate AHE in the DCDW phase, as in WSM. We shall see that the intrinsic contribution to AHE can be regarded as an “unquantized” version of the quantum Hall effect.

We can derive the Hall coefficient by way of the Kubo formula, considering a linear response to a tiny electric field [21]. For translational invariant systems, the Hall conductivity renders

$$\sigma_{xy} = e^2 \int \frac{d^3k}{(2\pi)^3} b_z(\mathbf{k}) f(E_k), \quad (9)$$

where $\mathbf{b}(\mathbf{k})$ is the Berry curvature in the momentum space, defined by the Berry connection $\mathbf{a}(\mathbf{k})$, $\mathbf{b}(\mathbf{k}) = \nabla_{\mathbf{k}} \times \mathbf{a}(\mathbf{k})$. Note that the factor e^2 comes from the cancellation due to the different directions of the wave vector for u and d quarks. Once the eigenfunctions $|u_k\rangle$ are known for any Hamiltonian $H(\mathbf{k})$, the Berry connection renders

$$\mathbf{a}(\mathbf{k}) = -i\langle u_k | \nabla_{\mathbf{k}} | u_k \rangle. \quad (10)$$

When Equation (9) is further rewritten as

$$\sigma_{xy} = \int \frac{dk_z}{2\pi} \left[e^2 \int \frac{d^2k}{(2\pi)^2} b_z(\mathbf{k}) f(E_k) \right], \quad (11)$$

where $f(E_k)$ is the Fermi-Dirac distribution function, we find that the formula in the parenthesis is the TKNN formula of 2D quantum Hall systems [22], where the Hall conductivity can be written as a momentum integral over the Brillouin zone,

$$\sigma_{xy}^{2D} = e^2 \sum_n \int_{BZ} \frac{d^2k}{(2\pi)^2} \left[\frac{\partial a_{n,y}}{\partial k_z} - \frac{\partial a_{n,z}}{\partial k_y} \right] \tag{12}$$

$$= \frac{e^2}{2\pi} \sum_n \nu_n. \tag{13}$$

where n denotes the band number and the integer ν_n is the first Chern number.

3.2. AHE in the DCDW Phase

Since the eigenenergy and eigenfunction are already obtained, it is straightforward to evaluate the Berry curvature in the DCDW phase. Then its z -component renders

$$b_{s,z} = \frac{-1}{2E_{\varepsilon=+1,s}^3} \left(sE_0 + \frac{q}{2} \right), \tag{14}$$

where $E_0 = \sqrt{p_z^2 + M^2}$ [20]. For $s = -1$, there appear two Weyl points at $\mathbf{p} = (0, 0, \pm K_0)$, and we can easily see that $\mathbf{b}_{s=-1}$ resembles the magnetic field produced by the Dirac monopole and antimonopole sitting at the Weyl points; indeed we can see that Equation (14) takes the approximate form, $b_{-1,z} \cong \mp \frac{p'_z}{2|\mathbf{p}'|^3}$ with $\mathbf{p}' = (p_x, p_y, p_z \pm K_0)$ around each Weyl point, $\mathbf{p} = (0, 0, \mp K_0)$.

Then, the contribution to the Hall conductivity from the Dirac sea can be evaluated as

$$\sigma_{xy}^{\text{Dirac}} = e^2 \sum_{s=\pm 1} \int \frac{d^3p}{(2\pi)^3} \frac{1}{2E_{\varepsilon=+1s}^3} (sE_0 + q/2). \tag{15}$$

The integral apparently diverges and depends on the cut-off scheme [23,24]. It is a subtle point; we must impose a physical condition to fix the finite term, which may be regarded as a kind of renormalization condition. The relevant condition for the DCDW phase is $\sigma_{xy}^{\text{Dirac}} \rightarrow 0$ as $M \rightarrow 0$, because AHE should vanish at the normal quark matter. This is achieved by using the gauge invariant regularizations such as the proper-time method or the heat-kernel method. Here, we apply the proper-time regularization (Figure 3 illustrates how the integral along p_z axis works),

$$\begin{aligned} \sigma_{xy}^{\text{Dirac}} &= \lim_{\Lambda \rightarrow \infty} \frac{e^2}{2\Gamma(3/2)} \sum_{s=\pm 1} \int \frac{d^3p}{(2\pi)^3} (sE_0 + q/2) \int_{\Lambda^{-2}}^{\infty} d\tau \tau^{1/2} e^{-\tau E_s^2} \\ &= \frac{e^2}{4\pi^2} \sum_{s=\pm 1} \int_0^{\infty} dp_z \text{sign}(sE_0 + q/2) \\ &\quad - \frac{e^2}{4\pi^{5/2}} \lim_{\Lambda \rightarrow \infty} \sum_{s=\pm 1} \int_0^{\infty} dp_z (sE_0 + q/2) \int_0^{\Lambda^{-2}} d\tau \tau^{-1/2} e^{-\tau (sE_0 + q/2)^2}. \end{aligned} \tag{16}$$

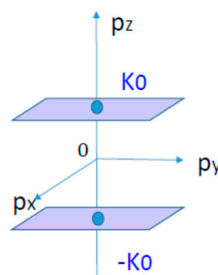


Figure 3. Integral along the p_z axis. The function $sE_0 + q/2$ changes its sign at the Weyl points for $s = -1$, while it is constant for $s = 1$.

The second term is evaluated to give $-e^2q/(2\pi)^2$, while the first term gives,

$$\frac{e^2}{4\pi^2}(2K_0). \quad (17)$$

One may find this is related to the topological quantity by rewriting it as

$$\int_{-K_0}^{K_0} \frac{dp_z}{2\pi} \left(\frac{e^2}{2\pi} \right), \quad (18)$$

where the quantity $e^2/2\pi$ is nothing else but the Hall conductivity for 2D quantum Hall systems with the Chern number $\nu = 1$. Thus, we can regard the DCDW phase as a stack of 2D quantum Hall systems to the 3rd direction [21]. Eventually, we find

$$\sigma_{xy}^{\text{Dirac}} = \frac{e^2}{4\pi^2}(2K_0 - q), \quad (19)$$

where we can easily check $\sigma_{xy}^{\text{Dirac}} \rightarrow 0$ as $M \rightarrow 0$, as it should be. Accordingly, the anomalous Hall current can be represented in the form $\mathbf{j}_{\text{AHE}}^{\text{Dirac}} = \frac{e^2}{(2\pi)^2} (1 - 2K_0/|\mathbf{q}|) \mathbf{q} \times \mathbf{E}$. It is to be noted that this expression is somewhat different for the one for Weyl semimetal, where the contribution from the valence band reads $(\sigma_{xy})_{\text{WSM}} = e^2K_0/2\pi^2$. This is because AHE is possible there even if $m = 0$.

4. Transport Properties in the Presence of the Magnetic Field

4.1. Hall Conductivity

The effective Hamiltonian for quasi-particles in the DCDW phase is given as

$$H_{\text{MF}} = \boldsymbol{\alpha} \cdot (\mathbf{p} - Q\mathbf{A}) + \beta M + \mathbf{q} \cdot \boldsymbol{\alpha} \gamma_5 \tau_3 / 2, \quad (20)$$

where $Q = \text{diag}(e_u, e_d)$ ($e_u = 2e/3$, $e_d = -e/3$), in the presence of the magnetic field. Since it has been shown that $\mathbf{q} \parallel \mathbf{B}$ is the most favorable configuration [25], we set magnetic field along z -axis without loss of generality. Then, the Kubo formula gives the formula of the Hall conductivity [26],

$$\sigma_{xy} = i \int_{-\infty}^{+\infty} f(\eta) A_{xy}(\eta) d\eta, \quad (21)$$

$$A_{xy}(\eta) = i \text{Tr} \left\{ Q^2 \left[j_x (dG^+ / d\eta) j_y \delta(\eta - H_{\text{MF}}) - j_x \delta(\eta - H_{\text{MF}}) j_y (dG^- / d\eta) \right] \right\},$$

where the Green functions are defined by $G^\pm(\eta) = (\eta - H_{\text{MF}} \pm i\varepsilon)^{-1}$, and the current operator j_a is given by $j_a = -i[r_a, H_{\text{MF}}] = \alpha_a$. Note that the TKNN formula is no longer useful in this case. Furthermore, we must carefully take into account the effect of an axial anomaly in the presence of the magnetic field. We then use the different approach from the previous section [27].

Streda has further rewritten Equation (21) into the following form [28],

$$\sigma_{xy} = \sigma_{xy}^{\text{I}} + \sigma_{xy}^{\text{II}}, \quad (22)$$

where the first term corresponds to the classical Drude-Zener result,

$$\sigma_{xy}^{\text{I}} = \frac{1}{2} i \text{Tr} \left\{ Q^2 \left[j_x G^+(\mu) j_y \delta(\mu - H) - j_x \delta(\mu - H) j_y G^-(\mu) \right] \right\}, \quad (23)$$

at $T = 0$, and the second term can be expressed by the use of the number of state $N^f(E)$ for each flavor to represent the quantum effect,

$$\sigma_{xy}^{\Pi} = -\sigma_{yx}^{\Pi} = \sum_f e_f \left. \frac{\partial N^f(E)}{\partial B} \right|_{E=\mu} . \tag{24}$$

The number of states below the energy E is defined by

$$\begin{aligned} N^f(E) &= \frac{1}{2} \int_{-\infty}^E \text{Tr}' \delta(\eta - H_{\text{MF}}) d\eta \\ &= N^f(0) + N_F^f(E), \end{aligned} \tag{25}$$

where Tr' means no summation in the flavor space. It consists of the contribution of the Dirac sea $N^f(0)$ and that of the Fermi sea $N_F^f(E)$. In the usual case, the first term gives no contribution and only the second term gives rise to the Hall conductivity. On the other hand, anomalous Hall conductivity just comes from the first term, when it is non-vanishing. We would like to demonstrate it.

4.2. Spectral Asymmetry and AHE

The effective Hamiltonian can be easily diagonalized [24] to give for each flavor f ,

$$\begin{aligned} E_{n,s,\varepsilon}^f(p_z) &= \varepsilon \sqrt{\left(s \sqrt{M^2 + p_z^2} - q/2 \right)^2 + 2|e_f|Bn}, \quad n = 1, 2, 3, \dots \\ E_{n=0,\varepsilon}(p_z) &= \varepsilon \sqrt{M^2 + p_z^2} - q/2 \end{aligned} \tag{26}$$

where $\varepsilon = \pm 1$ denotes the particle–antiparticle states, and $s = \pm 1$ specifies the spin degree of freedom (See Figure 4). Note that there is no spin degree of freedom for the lowest Landau level (LLL); there occurs dimensional reduction for LLL and the eigenspinor is represented by two components.

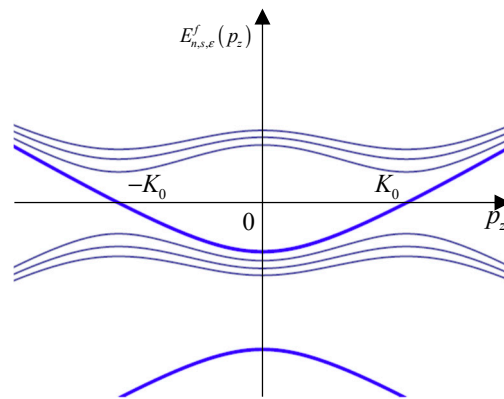


Figure 4. Energy spectra as functions of p_z . Thick lines denote the lowest Landau level (LLL).

One may immediately notice that the energy spectrum exhibits a peculiar feature: the spectrum for higher Landau levels with $n \neq 0$ is symmetric with respect to the level line, while that of the LLL is asymmetric. Such spectral asymmetry of the LLL gives rise to an interesting consequence. It has been shown [29] that such spectral asymmetry has a topological origin and is related to axial anomaly. Consequently, it gives anomalous baryon number in the DCDW phase and spreads the DCDW phase in the wide region in the QCD phase diagram in the presence of the magnetic field [25]. More interestingly, axial anomaly induces spontaneous magnetization in the DCDW phase [30], which in turn induces anomalous Hall current.

Writing the baryon number operator in the normal ordering form, $\hat{N}_f = \frac{1}{2} \int d^3x [\Psi_f^\dagger(x), \Psi_f(x)]$ ($f = u$ or d), we find $N(E) = N_{\text{norm}}(E) + N_{\text{anom}}$ by counting the number of the eigenstates below

energy E . The first term is the usual one and can be written as $N_{\text{norm}}(E) = \int_0^E \text{Tr}\delta(\lambda - H)d\lambda$ at $T = 0$. The quasi-particle density of states for the DCDW phase can be written as

$$D_{\text{DCDW}}^f(\lambda) = N_c \frac{|e_f|B}{(2\pi)^2} \sum_{\epsilon=\pm 1} \int_{-\infty}^{\infty} dp_z \left(\delta(\lambda - E_{n=0,\epsilon}(p_z)) + \sum_{s=\pm 1} \sum_{n=1}^{\infty} \delta(\lambda - E_{n,s,\epsilon}^f(p_z)) \right). \tag{27}$$

Thereby $N_{\text{norm}}(E)$ reads

$$N_{\text{norm}}(E) = \sum_f N_{\text{norm}}^f(E) = \sum_f \int_0^E D_{\text{DCDW}}^f(\lambda)d\lambda. \tag{28}$$

Thus, the contribution to the conductivity from the Fermi sea can be written as

$$\sigma_{xy}^{\text{Fermi}} = \sum_f e_f \left. \frac{\partial N_{\text{norm}}^f(E)}{\partial B} \right|_{E=\mu}. \tag{29}$$

The second term can be written as

$$N_{\text{anom}} = -\frac{1}{2} \int_{-\infty}^{+\infty} \text{sign}(\lambda) \text{Tr}\delta(\lambda - H)d\lambda. \tag{30}$$

We can see that it comes from the spectral asymmetry; it can also be represented in terms of the η invariant introduced by Atiyah–Patodi–Singer [31], $N_{\text{anom}} = -\frac{1}{2} \sum_f \eta_H^f$. The expression, Equation (30), is not well-defined as it is, and must be properly regularized to extract the physical result. Using Equation (26) and the following gauge-invariant regularization, we can evaluate the η invariant [29] for each flavor.

$$\begin{aligned} \eta_H^f &= \lim_{s \rightarrow 0^+} \frac{|e_f|B}{2\pi} N_c \int \frac{dp}{2\pi} \sum_{\epsilon} \text{sign}(E_{n=0,\epsilon}(p)) |E_{n=0,\epsilon}(p)|^{-s} \\ &= \begin{cases} N_c \frac{|e_f|Bq}{2\pi^2}, & M > \frac{q}{2} \\ N_c \frac{|e_f|Bq}{2\pi^2} - \frac{|e_f|B}{\pi^2} N_c \sqrt{\left(\frac{q}{2}\right)^2 - M^2}, & M < \frac{q}{2} \end{cases} \end{aligned} \tag{31}$$

Accordingly, the anomalous Hall conductivity can be given as

$$\begin{aligned} \sigma_{xy}^{\text{anom}} &= -\frac{1}{2} \sum_f e_f \frac{\partial \eta_H^f}{\partial B} \\ &= \begin{cases} -\frac{e^2 q}{4\pi^2} & M > \frac{q}{2} \\ \frac{e^2}{2\pi^2} \sqrt{\left(\frac{q}{2}\right)^2 - M^2} - \frac{e^2 q}{4\pi^2} & M < \frac{q}{2} \end{cases} \end{aligned} \tag{32}$$

where $N_c = 3$. This is the same result as the previous one, Equation (19), as it should be, but it is interesting to see the different manifestation of the topological effect in two calculations; one is given by the Berry curvature and Dirac monopole at the Weyl points, and the other by spectral asymmetry. It is to be noted again that our result is different from the one for WSM; some authors have obtained the different result [32]:

$$\sigma_{xy}^{\text{anom}} = \frac{e^2}{2\pi^2} \sqrt{b^2 - m^2}, \tag{33}$$

where $b > m$ by using the momentum cut-off regularization for WSM. However, as is already mentioned, the η invariant is given by the energy eigenstates, and gauge invariant regularizations must be used to obtain the relevant result.

It may be worth noting that for the quantized Hall effect in 2D Hall systems, $\sigma_{xy}^I = 0$, $\sigma_{xy}^{II} = -e^2 n / (2\pi)$ with n being the number of bands [28]. On the other hand, $\sigma_{xy}^{II} = 0$ in 3D Dirac materials with $b = 0$, and the whole contribution comes from σ_{xy}^I , $\sigma_{xy}^I \cong en_e / B$ with n_e being the electron number [13], provided that the effect of impurities can be neglected.

5. Summary and Concluding Remarks

We have discussed some topological aspects of the transport properties in the DCDW phase, in relation to WSM. Anomalous Hall conductivity is derived in two ways, using the Kubo formula. We have seen two different manifestations of the topological effect; one comes from the magnetic monopoles sitting at the Weyl points in the momentum space, and the other from the spectral asymmetry.

We have seen that the result of the anomalous Hall conductivity is different between our case and Weyl semimetal. The reason is unclear, but the boundary effect should probably be taken into account to understand this difference.

Many subjects are left for further consideration. First of all, we must clarify the boundary effect for the anomalous Hall effect. At the same time, we must clarify the role of axial anomaly in the presence of the magnetic field, since it should be closely related to the spectral asymmetry.

The interplay of the usual Hall effect and AHE in the magnetic field is an interesting and important subject, not only theoretically but also phenomenologically for compact stars, especially for magnetars.

It is interesting to extend the current framework to involve the CPT odd term, $\gamma_5 \boldsymbol{\gamma} \cdot \mathbf{b} \rightarrow \gamma_5 \gamma^\mu b_\mu$. Then, we can incorporate the chiral magnetic effect [33], where b_0 plays a role of chiral chemical potential μ_5 . It should also be interesting to study quantum phase transition between two cases, $b_0 > |\mathbf{b}|$ and $b_0 < |\mathbf{b}|$, from the literature [34].

The effect of the tiny but finite current mass must be elucidated beyond the chiral limit. It may be a rather hard task, since there have been no analytical solutions yet. It may become important near the phase boundary, especially around the Lifshitz point at finite temperature (see Figure 1). On the other hand, one can expect that the effect is small in the well-developed phase at low-temperature. This subject will be left for future exploration.

Since the electrical current and the thermal current are related to each other, one may discuss thermal conductivity using the Wiedemann–Franz law at low-temperature. It well holds for electrons in metals, but the deviations from the Wiedemann–Franz law are sometimes observed, e.g., in QCD matter [35], where $\bar{q}q$ fluctuations play the important roles. Therefore, we must carefully discuss thermal conductivity. We expect that the Wiedemann–Franz law well holds for anomalous Hall conductivity in the DCDW phase, at least in the well-developed phase, where mean-field approximation should work well. This subject will be discussed elsewhere.

Author Contributions: T.T. designed the program of whole study, and wrote initial draft of manuscript. H.A. contributed in giving an interpretation to the Hall conductivity, and assisted in the presentation of manuscript. All authors have read and agreed to the published version of the manuscript.

Funding: JSPS KAKENHI Grant Number JP19K03868.

Acknowledgments: One of the authors (T.T.) thanks the organizers for their hospitality during the conference “The Modern Physics of Compact Stars and Relativistic Gravity 2019”. The work of H.A. was supported by JSPS KAKENHI Grant Number JP19K03868.

Conflicts of Interest: The authors declare no conflicts of interest.

References

1. Friman, B.; Hoehne, C.; Knoll, J.; Leupold, S.; Randrup, J.; Rapp, R. The CBM Physics book. *Lect. Notes Phys.* **2011**, *814*, 1.
2. De Forcrand, P. Simulating QCD at finite density. *PoS LAT* **2009**, *2009*, 010.
3. Nakano, E.; Tatsumi, T. Chiral symmetry and density waves in quark matter. *Phys. Rev.* **2005**, *D71*, 114006. [[CrossRef](#)]

4. Nickel, D. How many phases meet at the chiral critical point? *Phys. Rev. Lett.* **2009**, *103*, 072301. [[CrossRef](#)]
5. Nickel, D. Inhomogeneous phases in the Nambu-Jona-Lasinio and quark-meson model. *Phys. Rev.* **2009**, *D80*, 074025. [[CrossRef](#)]
6. Buballa, M.; Carignano, S. Inhomogeneous chiral condensates. *Prog. Part. Nucl. Phys.* **2015**, *81*, 39. [[CrossRef](#)]
7. Tatsumi, T. Inhomogeneous Chiral Phase in Quark Matter. *JPS Conf. Proc.* **2018**, *20*, 011008.
8. Abuki, H. Chiral crystallization in an external magnetic background: Chiral spiral versus real kink crystal. *Phys. Rev.* **2018**, *D98*, 054006. [[CrossRef](#)]
9. Armitage, N.P.; Mele, E.J.; Vishwanath, A. Weyl and Dirac semimetals in three-dimensional solids. *Rev. Mod. Phys.* **2018**, *90*, 015001. [[CrossRef](#)]
10. Nagaosa, N.; Sinova, J.; Onoda, S.; MacDonald, A.H.; Ong, N.P. Anomalous Hall effect. *Rev. Mod. Phys.* **2010**, *82*, 1539. [[CrossRef](#)]
11. Xiao, D.; Chang, M.-C.; Niu, Q. Berry phase effects on electronic properties. *Rev. Mod. Phys.* **2010**, *82*, 1959. [[CrossRef](#)]
12. Potekhin, A.Y.; Pons, J.A.; Page, D. Neutron Stars-Cooling and Transport. *Space Sci. Rev.* **2015**, *191*, 239. [[CrossRef](#)]
13. Konye, V.; Ogata, M. Magnetoresistance of a three-dimensional Dirac gas. *Phys. Rev.* **2018**, *B98*, 195420. [[CrossRef](#)]
14. Karasawa, S.; Tatsumi, T. Variational approach to the inhomogeneous chiral phase in quark matter. *Phys. Rev.* **2015**, *D92*, 116004. [[CrossRef](#)]
15. Baser, G.; Dunne, G.V. Twisted kink crystal in the chiral Gross-Neveu model. *Phys. Rev.* **2008**, *D78*, 065002.
16. Basar, G.; Dunne, G.V.; Thies, M. Inhomogeneous condensates in the thermodynamics of the chiral NJL2 model. *Phys. Rev.* **2009**, *D79*, 105012.
17. Fulde, P.; Ferrel, R.A. Superconductivity in a strong spin-exchange field. *Phys. Rev.* **1964**, *135*, A550. [[CrossRef](#)]
18. Larkin, A.L.; Ovchinnikov, Y.N. Inhomogeneous state of superconductors. *Sov. Phys. JETP* **1965**, *20*, 762.
19. Wilczek, F. Two applications of axion electrodynamics. *Phys. Rev. Lett.* **1987**, *58*, 1799. [[CrossRef](#)]
20. Ferrer, E.J.; de la Incera, V. Dissipationless Hall current in dense quark matter in a magnetic field. *Phys. Lett.* **2017**, *B769*, 208. [[CrossRef](#)]
21. Tatsumi, T.; Yoshiike, R.; Kashiwa, K. Anomalous Hall effect in dense QCD matter. *Phys. Lett.* **2018**, *B785*, 46. [[CrossRef](#)]
22. Thouless, D.J.; Kohmoto, M.; Nightingale, M.P.; den Nijs, M. Quantised Hall Conductance in a two-dimensional periodic potential. *Phys. Rev. Lett.* **1982**, *49*, 405. [[CrossRef](#)]
23. Grushin, A.G. Consequences of a condensed matter realization of Lorentz-violating QED in Weyl semi-metals. *Phys. Rev.* **2012**, *D86*, 045001. [[CrossRef](#)]
24. Goswami, P.; Tewari, S. Axionic field theory of (3+1)-dimensional Weyl semimetals. *Phys. Rev.* **2013**, *B88*, 245107. [[CrossRef](#)]
25. Frolov, I.E.; Zhukivsky, V.C.; Klimenko, G.K. Chiral density waves in quark matter within the Nambu-Jona-Lasinio model in an external magnetic field. *Phys. Rev.* **2010**, *D82*, 076002. [[CrossRef](#)]
26. Bastin, A.; Lewiner, C.; Betbeder-Matibet, O.; Nozieres, P. Quantum oscillations of the Hall effect of a Fermion gas with random impurity scattering. *J. Phys. Chem, Solids* **1971**, *32*, 1811. [[CrossRef](#)]
27. Tatsumi, T.; Abuki, H. Hall effect in the inhomogeneous chiral phase. **2020**. (in preparation).
28. Streda, P. Theory of quantized Hall conductivity in two dimensions. *J. Phys.* **1982**, *C15*, L717.
29. Tatsumi, T.; Nishiyama, K.; Karasawa, S. Novel Lifshitz point for chiral transition in the magnetic field. *Phys. Lett.* **2015**, *B743*, 66. [[CrossRef](#)]
30. Yoshiike, R.; Nishiyama, K.; Tatsumi, T. Spontaneous magnetization of quark matter in the inhomogeneous chiral phase. *Phys. Lett.* **2015**, *B751*, 123. [[CrossRef](#)]
31. Niemi, A.J.; Semenoff, G.W. Fermion number fractionization in quantum field theory. *Phys. Rept.* **1986**, *135*, 99. [[CrossRef](#)]
32. Zyuzin, A.A.; Burkov, A.A. Topological response in Weyl semimetals and the chiral anomaly. *Phys. Rev.* **2012**, *B86*, 115133. [[CrossRef](#)]
33. Fukushima, K.; Khazrizeev, D.E.; Warringa, H.J. Chiral magnetic effect. *Phys. Rev.* **2008**, *D78*, 074033. [[CrossRef](#)]

34. Klinkhamer, F.R.; Volovik, G.E. Emergent CPT violation from the splitting of Fermi points. *Int. J. Mod. Phys.* **2005**, *A20*, 2795. [[CrossRef](#)]
35. Harutyunyan, A.; Rischke, D.H.; Sedrakian, A. Transport coefficients of two-flavor quark matter from the Kubo formalism. *Phys. Rev.* **2017**, *D95*, 114021. [[CrossRef](#)]



© 2020 by the authors. Licensee MDPI, Basel, Switzerland. This article is an open access article distributed under the terms and conditions of the Creative Commons Attribution (CC BY) license (<http://creativecommons.org/licenses/by/4.0/>).